

# All-solid-state Li-metal cell using nanocomposite TiO<sub>2</sub> /polymer electrolyte and self-standing LiFePO<sub>4</sub> cathode

Asia Patriarchi<sup>1</sup>, Hamideh Darjazi<sup>2,3</sup>, Luca Minnetti<sup>1</sup>, Leonardo Sbrascini<sup>1</sup>, Giuseppe Antonio Elia<sup>2,3</sup>, Vincenzo Castorani<sup>4</sup>, Miguel Ángel Muñoz-Márquez<sup>1,3</sup>, Francesco Nobili<sup>1,3,\*</sup>

<sup>1</sup> *Chemistry Division , School of Science and Technology, University of Camerino, Via Madonna delle Carceri-ChIP, 62032 Camerino, MC, Italy; asia.patriarchi@unicam.it (A.P.); luca.minnetti@unicam.it (L.M.); leonardo.sbrascini@unicam.it (L.S.); miguel.munoz@unicam.it (M.Á.M.-M.)*

<sup>2</sup> *GAME Lab, Department of Applied Science and Technology (DISAT), Politecnico di Torino, Corso Duca degli Abruzzi 24, 10129 Torino, TO, Italy; hamideh.darjazi@polito.it (H.D.); giuseppe.elia@polito.it (G.A.E.)*

<sup>3</sup> *National Reference Center for Electrochemical Energy Storage (GISEL) – INSTM, Via Giusti 9, 50121 Firenze, FI, Italy*

<sup>4</sup> *HP Composites S.p.A., Via del Lampo, sn, Zona Ind.le Campolungo, 63100 Ascoli Piceno, AP, Italy; v.castorani@hpcomposites.it*

\* *Correspondence: francesco.nobili@unicam.it; Tel.: +39-0737-402216*

## Supporting Information

**Table S1:** Electrolyte resistance ( $R_e$ ), interphase resistance ( $R_i$ ), and chi-square value indicating the accuracy ( $\chi^2$ ) of the non-linear least squares (NLLS) analysis using the equivalent circuit  $R_e(R_1C_1)(R_2C_2)Q_w$  on the EIS data of the symmetrical Li/membrane/Li cells with different polymer-to-salt ratio (EO/Li), collected at OCV of the cells and after 25 hours. See Figure 1b,d in the manuscript for related Nyquist plots.

	<b>Cell Condition</b>	<b><math>R_e</math> (<math>\Omega</math>)</b>	<b><math>R_i = R_1 + R_2</math> (<math>\Omega</math>)</b>	<b><math>R = R_e + R_i</math> (<math>\Omega</math>)</b>	<b><math>\chi^2</math></b>
EO/Li 18:1	OCV	$18.7 \pm 0.2$	$190 \pm 11$	$209 \pm 11$	$2 \times 10^{-5}$
	After 25 hours	$3.6 \pm 0.6$	$448 \pm 6$	$452 \pm 6$	$1 \times 10^{-5}$
EO/Li 21:1	OCV	$11.0 \pm 0.4$	$125 \pm 6$	$136 \pm 6$	$4 \times 10^{-5}$
	After 25 hours	$13.3 \pm 0.3$	$178 \pm 11$	$191 \pm 11$	$3 \times 10^{-5}$
EO/Li 25:1	OCV	$10 \pm 2$	$776 \pm 13$	$786 \pm 13$	$2 \times 10^{-5}$
	After 25 hours	$24.3 \pm 0.3$	$929 \pm 8$	$953 \pm 8$	$1 \times 10^{-5}$

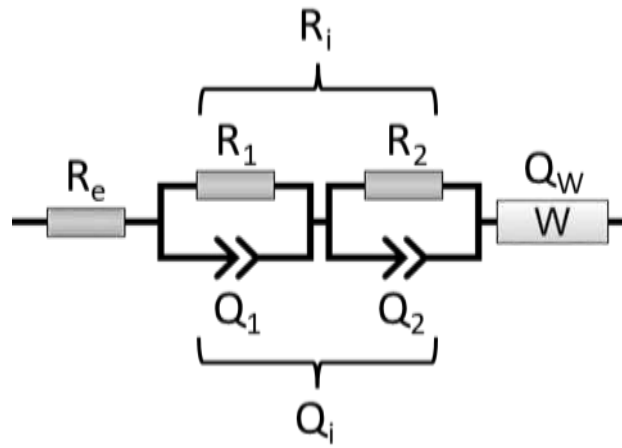


*Figure S1: Representation of the equivalent circuit used in Figure 1b,d.*

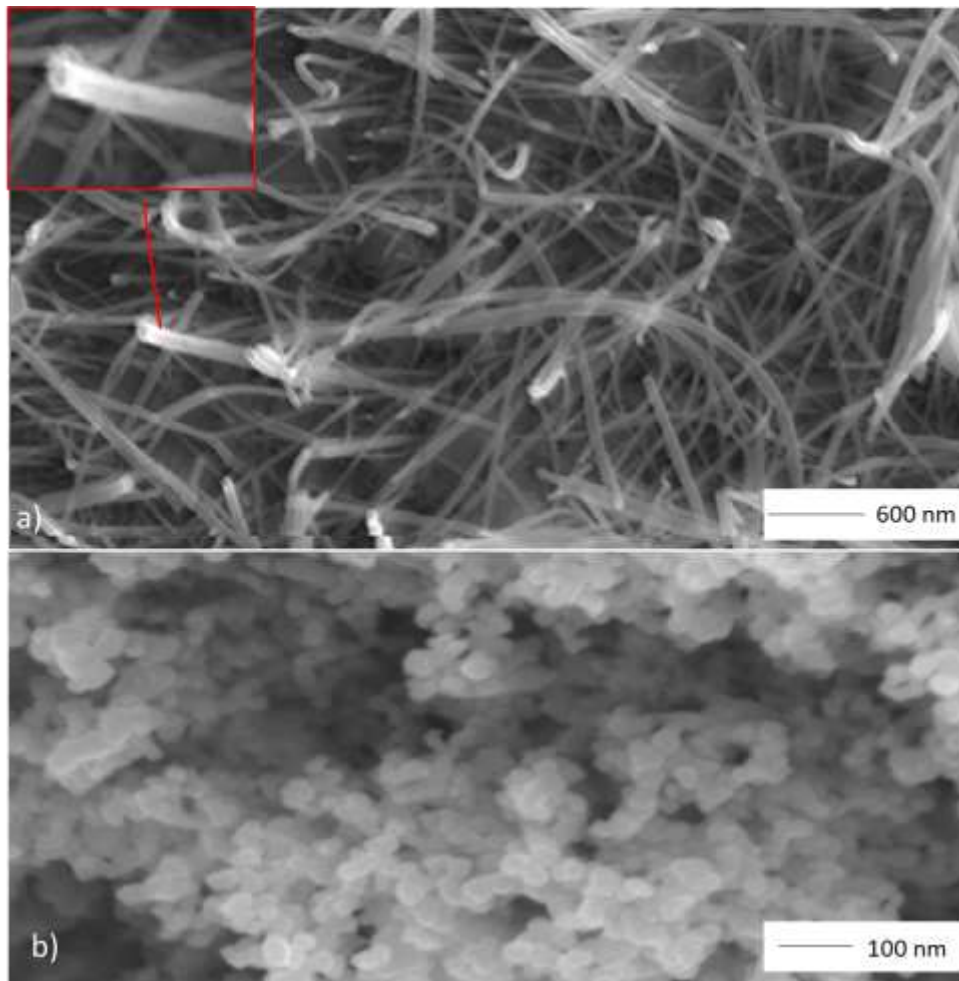


*Figure S2: SEM images of (a) synthesized titanium dioxide nanotubes and (b) commercial P25 nanoparticles.*

**Table S2:** Electrolyte resistance ( $R_e$ ), interphase resistance ( $R_i$ ), and chi-square value indicating the accuracy ( $\chi^2$ ) of the non-linear least squares (NLLS) analysis using the equivalent circuit  $R_e(R_1C_1)(R_2C_2)Q_w$  on the EIS data of the symmetrical Li/membrane/Li cells with  $TiO_2$  filler with different morphologies (nanotubes or nanoparticles) and concentration, collected at OCV of the cells and after 25 hours. See Figure 3 in the manuscript for related Nyquist plots.

	Filler Concentration	Cell Condition	$R_e$ ( $\Omega$ )	$R_i = R_1 + R_2$ ( $\Omega$ )	$\chi^2$
Nanoparticles	NP15	OCV	$17.0 \pm 0.3$	$193 \pm 14$	$2 \times 10^{-5}$
		After 25 hours	$13.2 \pm 0.2$	$445 \pm 34$	$1 \times 10^{-5}$
	NP10	OCV	$22.8 \pm 0.9$	$78 \pm 8$	$2 \times 10^{-5}$
		After 25 hours	$18.3 \pm 0.3$	$209 \pm 18$	$2 \times 10^{-5}$
	NP3	OCV	$22.8 \pm 0.2$	$380 \pm 10$	$7 \times 10^{-6}$
		After 25 hours	$16.6 \pm 0.2$	$437 \pm 9$	$8 \times 10^{-6}$
Nanotubes	NT15	OCV	$41.8 \pm 0.2$	$103 \pm 4$	$1 \times 10^{-5}$
		After 25 hours	$25.9 \pm 0.9$	$155 \pm 11$	$5 \times 10^{-5}$
	NT10	OCV	$21.1 \pm 0.3$	$73 \pm 4$	$1 \times 10^{-5}$
		After 25 hours	$16.4 \pm 0.3$	$91 \pm 5$	$2 \times 10^{-5}$
	NT3	OCV	$34.5 \pm 0.6$	$254 \pm 8$	$7 \times 10^{-6}$
		After 25 hours	$21.6 \pm 0.5$	$400 \pm 10$	$1 \times 10^{-5}$

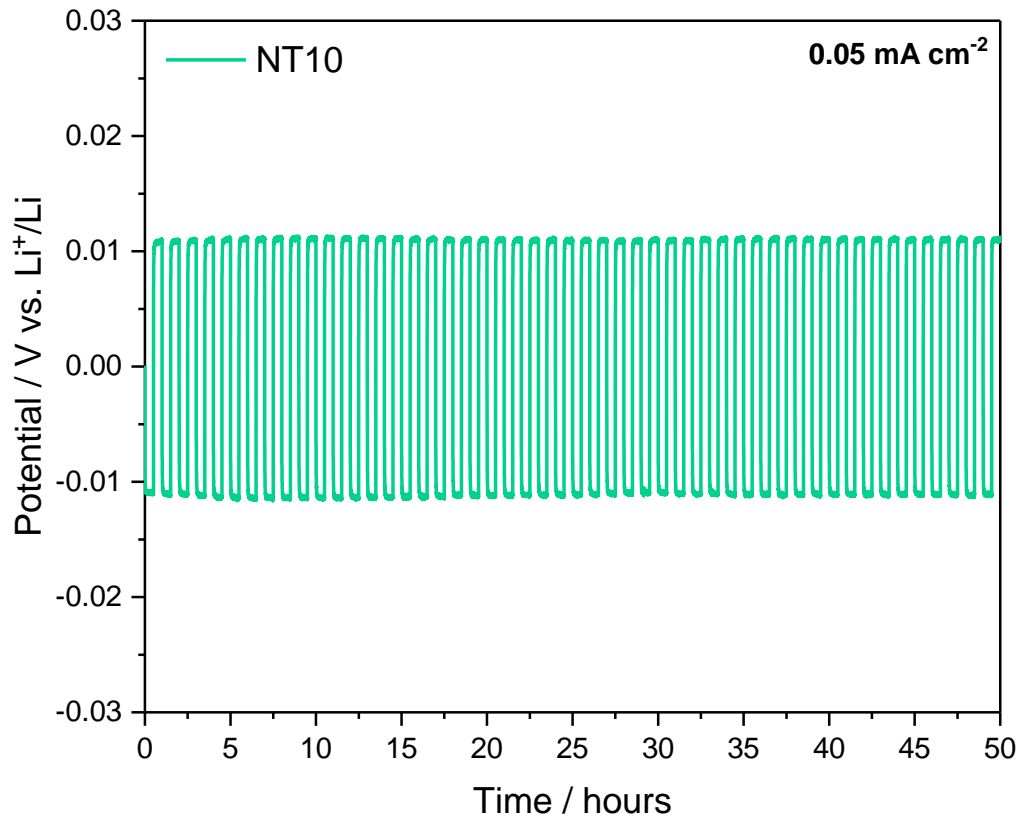


*Figure S3: 50 hours of galvanostatic plating/stripping test performed on symmetrical Li/NT10/Li cells.  $I = 0.05 \text{ mA cm}^{-2}$ ;  $T = 65 \text{ }^\circ\text{C}$ .*

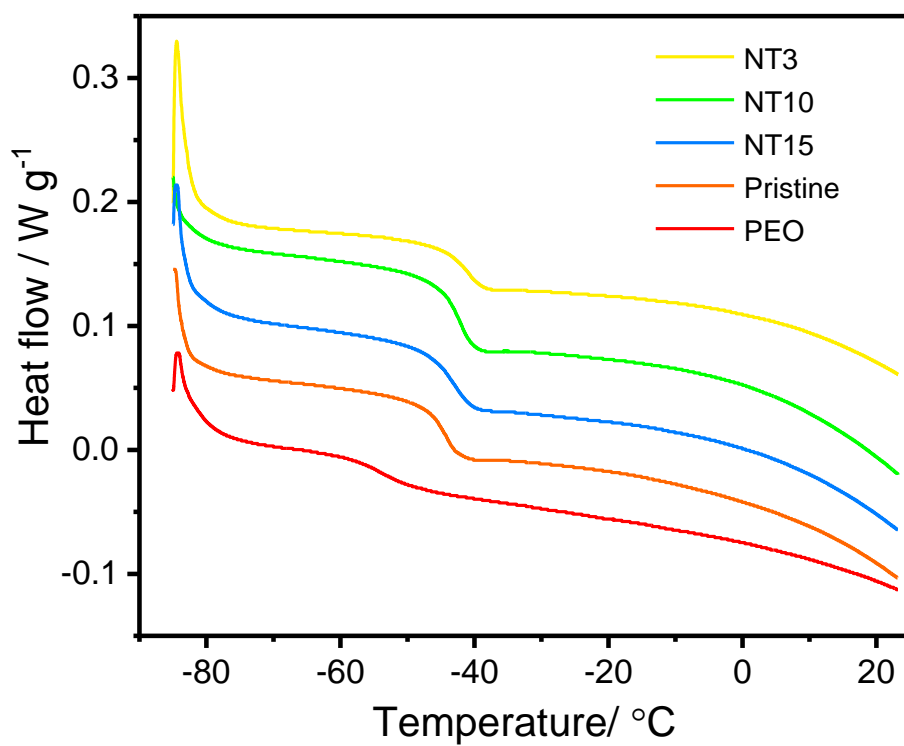


*Figure S4:* Differential Scanning Calorimetry curves of PEO polymer (red), pristine membrane (orange), NT15 (blue), NT10 (green), and NT3 (yellow) recorded under nitrogen flow in the -80 – 25  $^{\circ}\text{C}$  temperature range.

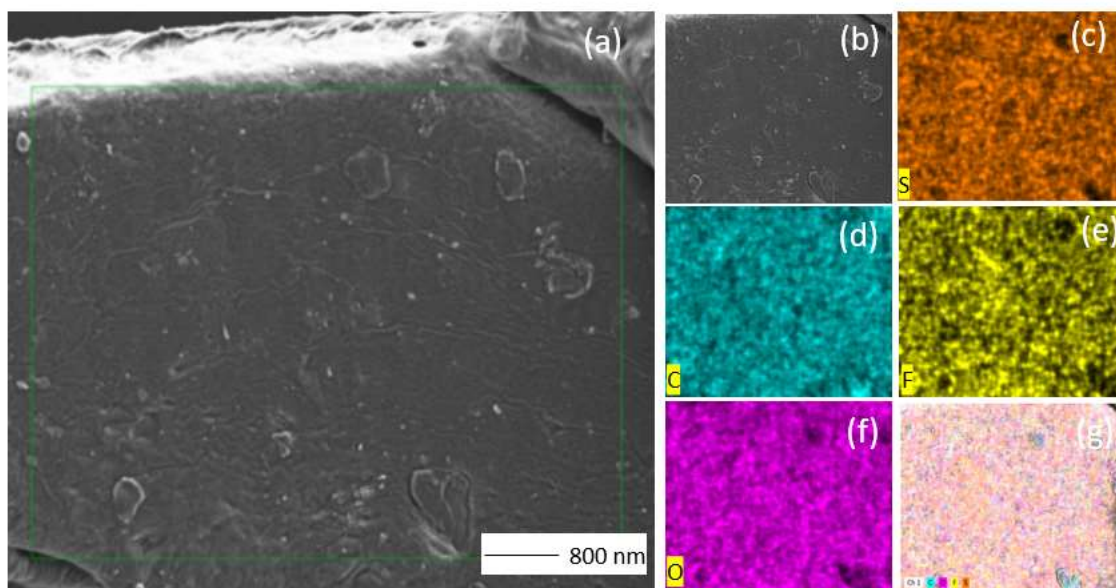


*Figure S5: (a) SEM image of the pristine membrane, (b) EDS mapping of (c) sulfur (d) carbon (e) fluorine and (f) oxygen. (g) Overlapping of all the elements detected by EDS.*

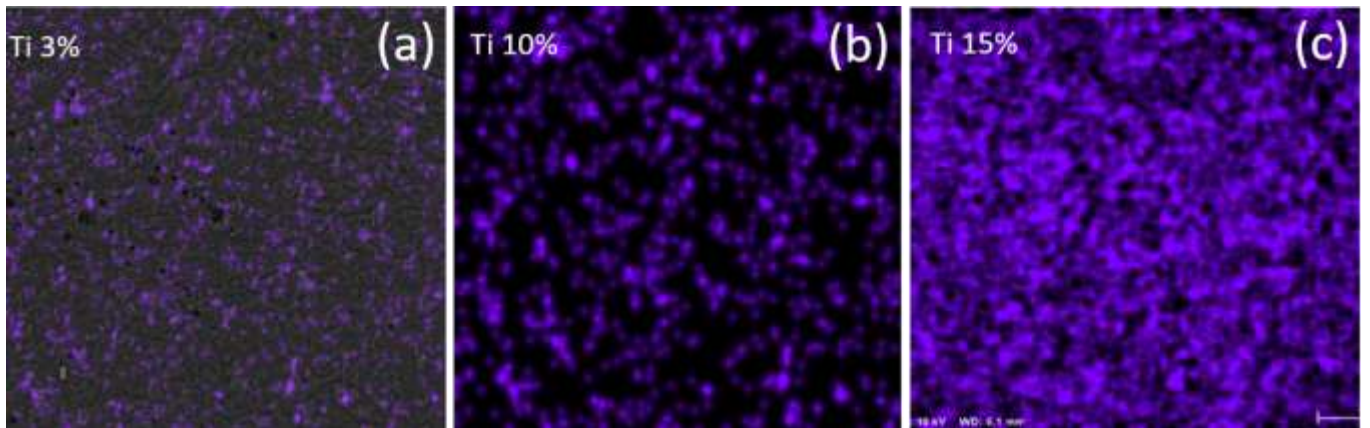


*Figure S6: EDS elemental maps of different concentrations of TiO<sub>2</sub> in (a) NT3, (b) NT10, and (c) NT15.*

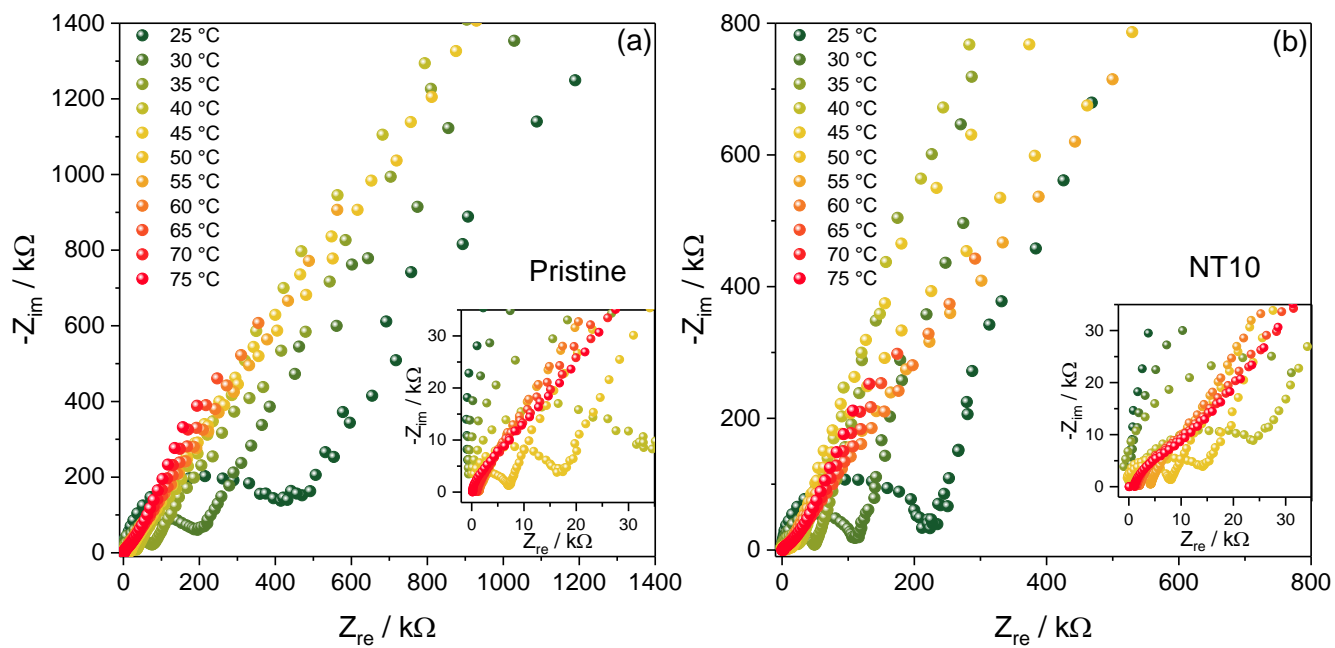


**Figure S7:** Nyquist plots related to EIS measurements performed at various temperatures on a stainless-steel/membrane/stainless-steel symmetrical cell with (a) pristine membrane and (b) NT10 to evaluate the electrolyte ionic conductivity, with magnification of the high-frequency region in the insets.

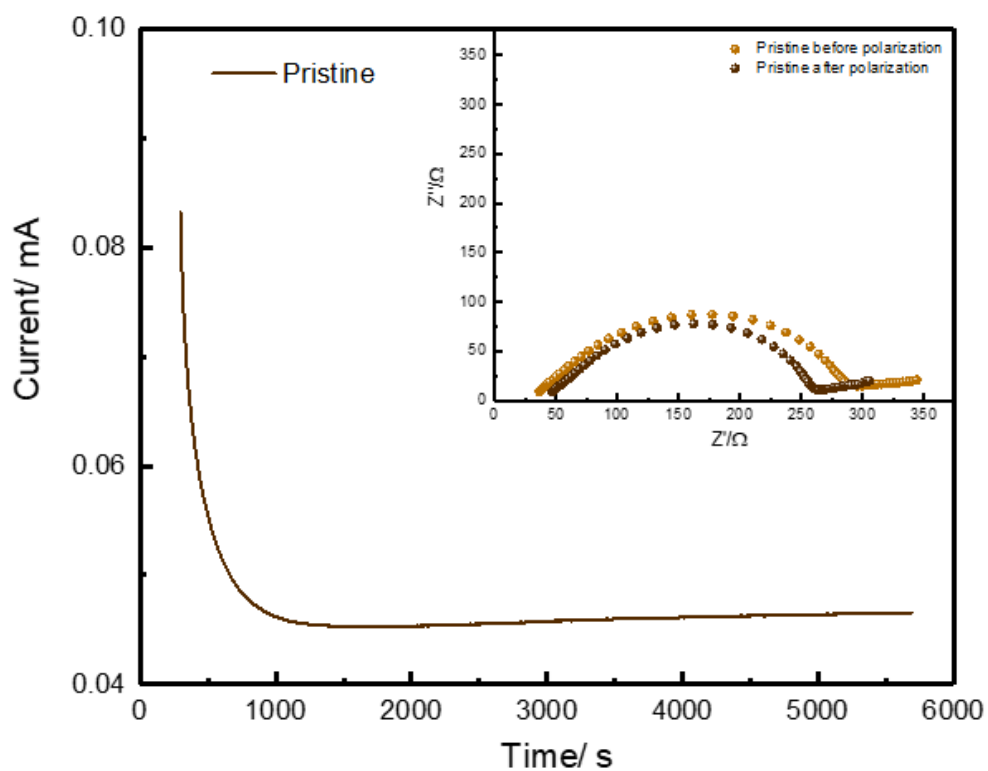


*Figure S8: Chronoamperometry curve recorded on a Li/Li symmetrical cell using pristine membrane as electrolyte for determination of  $\text{Li}^+$  transference number at 65 °C. The inset displays the corresponding Nyquist plots obtained by EIS at the initial and steady state.*

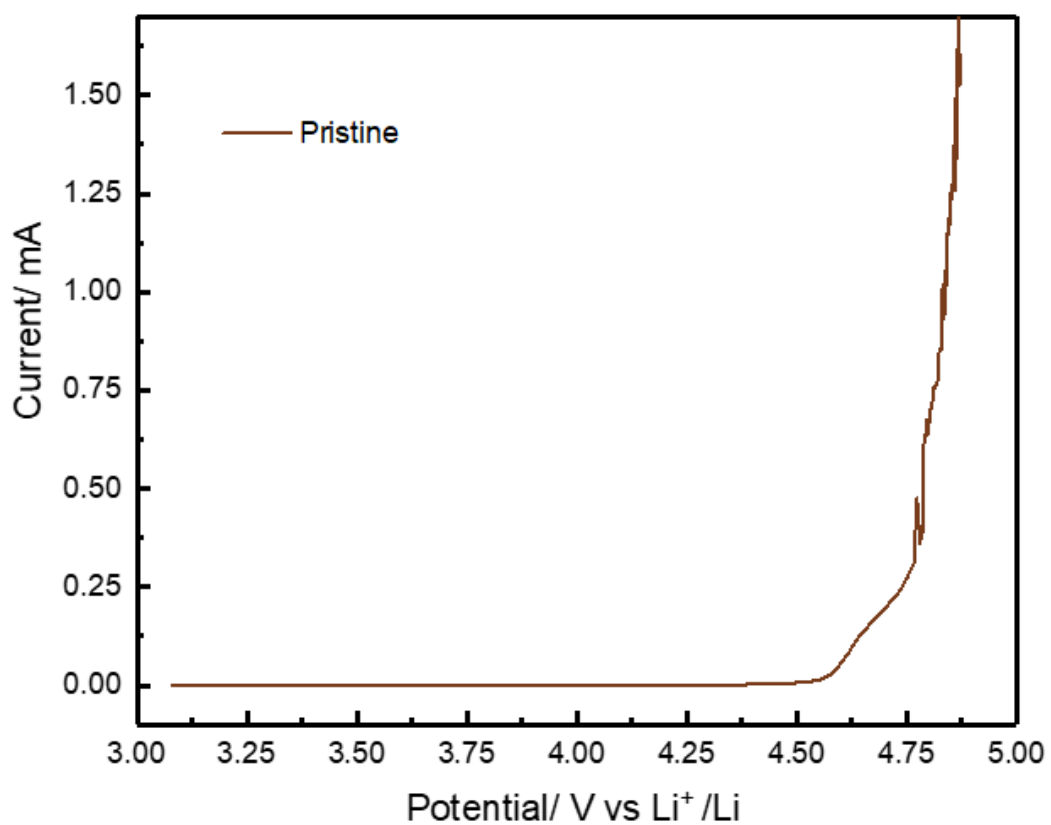


*Figure S9: Linear sweep voltammetry in anodic region (OCV – 5 V vs. Li<sup>+</sup>/Li potential range) performed at 65 °C in lithium cell using the pristine membrane as the electrolyte and Super P carbon coated on aluminium as the working electrode.*

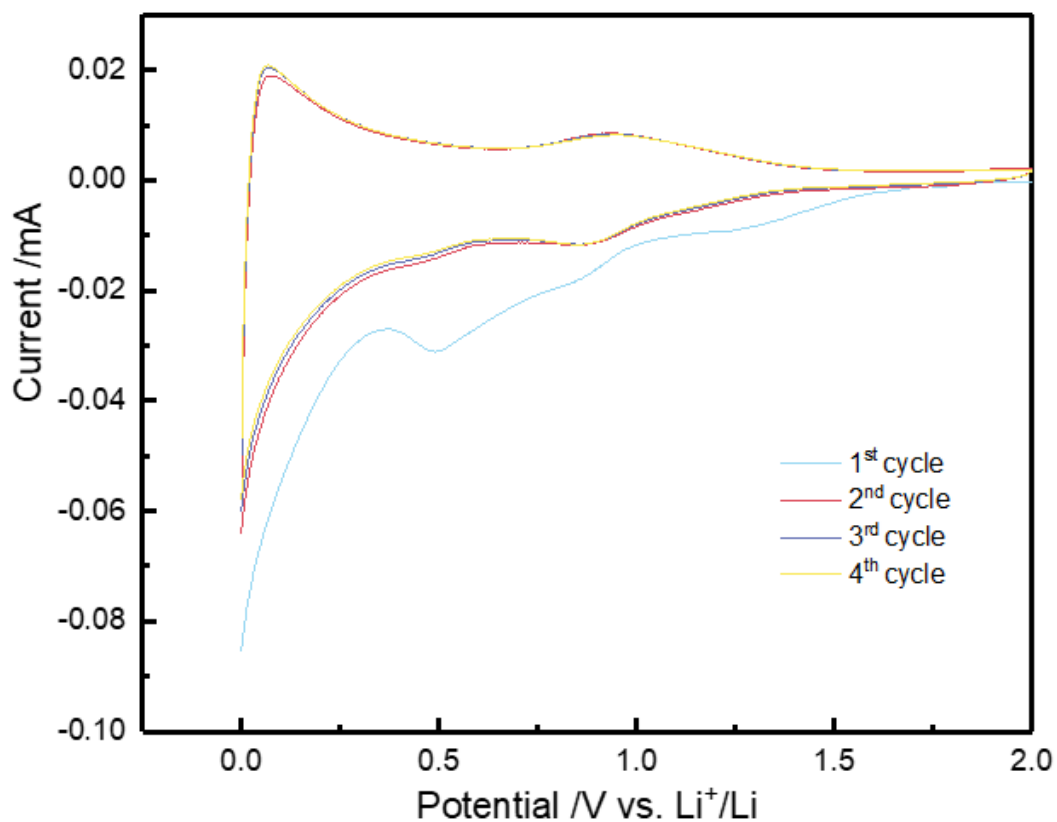


*Figure S10: CV curve of the cathodic region (0.01 – 2 V vs. Li<sup>+</sup>/Li potential range) performed at 65 ° using the NT10 membrane as the electrolyte and Super P carbon coated on copper as the working electrode.*

**Table S3:** NLLS analysis on the Nyquist plots reported in Figure 7d in the manuscript collected by EIS on a Li/NT10/Li symmetrical cell upon aging. The NLLS fitting was performed through the RelaxIS3 software, and the corresponding resistance trend is shown in Figure 7e in the manuscript.

Cell Condition	Equivalent Circuit	$R_i = R_1 + R_2 (\Omega)$	$\chi^2$
After 1 hour	$R_e(R_1C_1)(R_2C_2)Q_w$	90	$3 \times 10^{-5}$
After 3 hours	$R_e(R_1C_1)(R_2C_2)Q_w$	95	$6 \times 10^{-6}$
After 8 hours	$R_e(R_1C_1)(R_2C_2)Q_w$	102	$5 \times 10^{-6}$
After 20 hours	$R_e(R_1C_1)(R_2C_2)Q_w$	108	$7 \times 10^{-6}$
After 32 hours	$R_e(R_1C_1)(R_2C_2)Q_w$	104	$7 \times 10^{-6}$
After 2 days	$R_e(R_1C_1)(R_2C_2)Q_w$	103	$7 \times 10^{-6}$
After 2.5 days	$R_e(R_1C_1)(R_2C_2)Q_w$	104	$7 \times 10^{-6}$
After 3 days	$R_e(R_1C_1)(R_2C_2)Q_w$	103	$2 \times 10^{-5}$
After 3.5 days	$R_e(R_1C_1)(R_2C_2)Q_w$	100	$2 \times 10^{-5}$
After 4 days	$R_e(R_1C_1)(R_2C_2)Q_w$	99	$8 \times 10^{-6}$
After 4.5 days	$R_e(R_1C_1)(R_2C_2)Q_w$	98	$6 \times 10^{-6}$
After 5 days	$R_e(R_1C_1)(R_2C_2)Q_w$	99	$9 \times 10^{-6}$
After 5.5 days	$R_e(R_1C_1)(R_2C_2)Q_w$	98	$1 \times 10^{-5}$
After 6 days	$R_e(R_1C_1)(R_2C_2)Q_w$	98	$1 \times 10^{-5}$
After 6.5 days	$R_e(R_1C_1)(R_2C_2)Q_w$	97	$1 \times 10^{-5}$
After 7 days	$R_e(R_1C_1)(R_2C_2)Q_w$	96	$1 \times 10^{-5}$
After 7.5 days	$R_e(R_1C_1)(R_2C_2)Q_w$	96	$1 \times 10^{-5}$
After 8 days	$R_e(R_1C_1)(R_2C_2)Q_w$	95	$9 \times 10^{-6}$
After 8.5 days	$R_e(R_1C_1)(R_2C_2)Q_w$	94	$1 \times 10^{-5}$
After 9 days	$R_e(R_1C_1)(R_2C_2)Q_w$	95	$1 \times 10^{-5}$
After 9.5 days	$R_e(R_1C_1)(R_2C_2)Q_w$	95	$9 \times 10^{-6}$
After 10 days	$R_e(R_1C_1)(R_2C_2)Q_w$	96	$9 \times 10^{-6}$
After 10.5 days	$R_e(R_1C_1)(R_2C_2)Q_w$	97	$9 \times 10^{-6}$
After 11 days	$R_e(R_1C_1)(R_2C_2)Q_w$	98	$9 \times 10^{-6}$
After 11.5 days	$R_e(R_1C_1)(R_2C_2)Q_w$	99	$8 \times 10^{-6}$
After 12 days	$R_e(R_1C_1)(R_2C_2)Q_w$	100	$9 \times 10^{-6}$
After 12.5 days	$R_e(R_1C_1)(R_2C_2)Q_w$	101	$8 \times 10^{-6}$
After 13 days	$R_e(R_1C_1)(R_2C_2)Q_w$	103	$8 \times 10^{-6}$
After 13.5 days	$R_e(R_1C_1)(R_2C_2)Q_w$	104	$8 \times 10^{-6}$
After 14 days	$R_e(R_1C_1)(R_2C_2)Q_w$	105	$8 \times 10^{-6}$
After 14.5 days	$R_e(R_1C_1)(R_2C_2)Q_w$	107	$8 \times 10^{-6}$
After 15 days	$R_e(R_1C_1)(R_2C_2)Q_w$	110	$1 \times 10^{-5}$
After 15.5 days	$R_e(R_1C_1)(R_2C_2)Q_w$	110	$7 \times 10^{-6}$
After 16 days	$R_e(R_1C_1)(R_2C_2)Q_w$	112	$7 \times 10^{-6}$
After 16.5 days	$R_e(R_1C_1)(R_2C_2)Q_w$	114	$7 \times 10^{-6}$
After 17 days	$R_e(R_1C_1)(R_2C_2)Q_w$	115	$7 \times 10^{-6}$
After 17.5 days	$R_e(R_1C_1)(R_2C_2)Q_w$	117	$7 \times 10^{-6}$
After 18 days	$R_e(R_1C_1)(R_2C_2)Q_w$	118	$7 \times 10^{-6}$
After 18.5 days	$R_e(R_1C_1)(R_2C_2)Q_w$	120	$5 \times 10^{-6}$
After 19 days	$R_e(R_1C_1)(R_2C_2)Q_w$	122	$5 \times 10^{-6}$
After 19.5 days	$R_e(R_1C_1)(R_2C_2)Q_w$	123	$5 \times 10^{-6}$

After 20 days	$R_e(R_1C_1)(R_2C_2)Q_w$	125	$5 \times 10^{-6}$
After 20.5 days	$R_e(R_1C_1)(R_2C_2)Q_w$	128	$4 \times 10^{-6}$

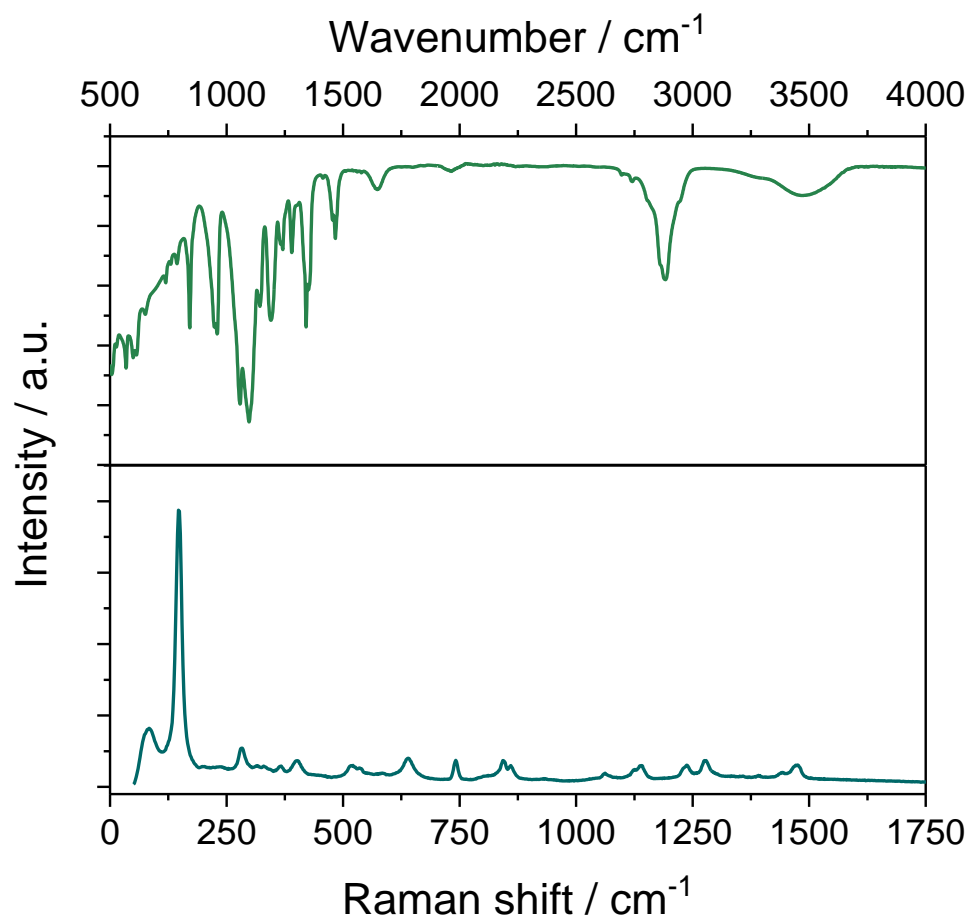


*Figure S11: IR spectrum (top panel), recorded in the 500 – 4000 cm<sup>-1</sup> range, and Raman spectrum (bottom panel), recorded in the 0 – 1750 cm<sup>-1</sup> range, of the NT10.*

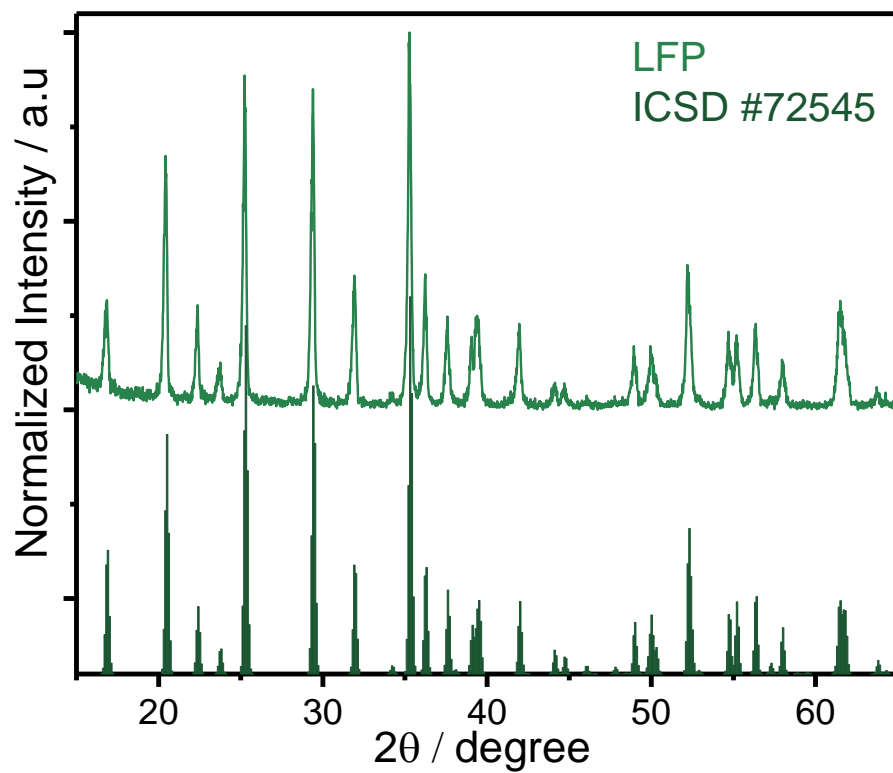


*Figure S12: XRD pattern of commercial LFP powder compared to corresponding reference diffractogram (ICSD #72545).*

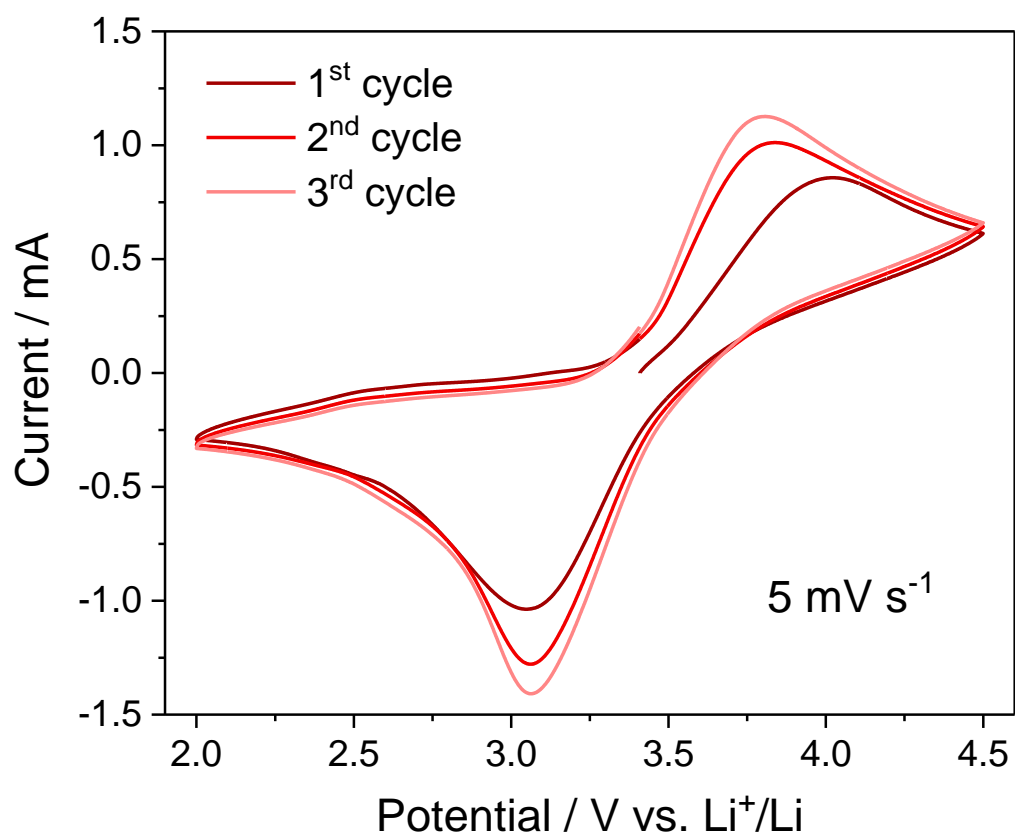


*Figure S13: CV measurement performed on the Li/NT10/SS\_LFP cell in the potential range 2.5 – 4.5 V vs. Li<sup>+</sup>/Li at the scan rate of 5 mV s<sup>-1</sup>.*